

Review

# Ultrasound and Photoacoustic Imaging of Laser-Activated Phase-Change Perfluorocarbon Nanodroplets

Heechul Yoon 

School of Electronics and Electrical Engineering, Dankook University, Yongin-si 16890, Korea; heechul.yoon@dankook.ac.kr

**Abstract:** Laser-activated perfluorocarbon nanodroplets (PFCnDs) are emerging phase-change contrast agents that showed promising potential in ultrasound and photoacoustic (US/PA) imaging. Unlike monophasic gaseous microbubbles, PFCnDs shift their state from liquid to gas via optical activation and can provide high US/PA contrast on demand. Depending on the choice of perfluorocarbon core, the vaporization and condensation dynamics of the PFCnDs are controllable. Therefore, these configurable properties of activation and deactivation of PFCnDs are employed to enable various imaging approaches, including contrast-enhanced imaging and super-resolution imaging. In addition, synchronous application of both acoustic and optical pulses showed a promising outcome vaporizing PFCnDs with lower activation thresholds. Furthermore, due to their sub-micrometer size, PFCnDs can be used for molecular imaging of extravascular tissue. PFCnDs can also be an effective therapeutic tool. As PFCnDs can carry therapeutic drugs or other particles, they can be used for drug delivery, as well as photothermal and photodynamic therapies. Blood barrier opening for neurological applications was recently demonstrated with optically-triggered PFCnDs. This paper specifically focuses on the activation and deactivation properties of laser-activated PFCnDs and associated US/PA imaging approaches, and briefly discusses their theranostic potential and future directions.

**Keywords:** perfluorocarbon nanodroplets; phase-change contrast agents; optical activation; ultrasound imaging; photoacoustic imaging



**Citation:** Yoon, H. Ultrasound and Photoacoustic Imaging of Laser-Activated Phase-Change Perfluorocarbon Nanodroplets. *Photonics* **2021**, *8*, 405. <https://doi.org/10.3390/photonics8100405>

Received: 30 July 2021

Accepted: 17 September 2021

Published: 22 September 2021

**Publisher's Note:** MDPI stays neutral with regard to jurisdictional claims in published maps and institutional affiliations.



**Copyright:** © 2021 by the author. Licensee MDPI, Basel, Switzerland. This article is an open access article distributed under the terms and conditions of the Creative Commons Attribution (CC BY) license (<https://creativecommons.org/licenses/by/4.0/>).

## 1. Introduction

Over the past decade, phase-change contrast agents were rigorously studied and showed promising outcomes in diagnostic ultrasound imaging and therapeutic applications [1–6]. These contrast agents consisting of a liquid perfluorocarbon (PFC) core, referred to as perfluorocarbon nanodroplets (PFCnDs), undergo a phase transition from liquid to gaseous state in response to an external trigger [7,8]. Ultrasound energy (or optical energy for laser activation of PFCnDs with a photo-absorber) can be applied to induce vaporization of PFCnDs, capable of providing on-demand controllable contrast. Unlike micrometer-sized gaseous bubbles, these liquid PFCnDs can be stably generated in a broad range of sizes down to a few hundred nanometers and remain stable in blood circulation [9,10]. Thus, applications of the PFCnDs are not necessarily limited to the vascular space [11,12]. Before activation, the administered PFCnDs could be small enough to extravasate through the leaky cancerous neovasculature for extravascular cancer imaging.

Incorporating an optical absorber into PFCnDs could offer another opportunity as a dual-modality agent, referred to as laser-activated PFCnDs, for ultrasound and photoacoustic (US/PA) imaging [5,10,13–15]. The characteristics of laser pulse for optical activation vary based on clinical needs. For example, a laser pulse with a wavelength of 1064 nm is generally preferred for deeper activation of PFCnDs, and its pulse duration typically ranges from 5–7 nanoseconds to induce the photoacoustic effect. The optical fluence irradiated to tissue with PFCnDs should follow the American National Standards

Institute safety limit for safe in vivo imaging ( $100 \text{ mJ}/\text{cm}^2$  for 1064-nm wavelength) [16]. The optically-triggered PFCnDs consist of a photo-absorber (optical dyes or nanoparticles), liquid perfluorocarbon, and surfactant shell, as illustrated in Figure 1. These three components of the laser-activated PFCnDs are essential design parameters determining major characteristics of the agents [12,14,17]. Corresponding to the clinical application of interest, they should be reasonably selected. For example, optical wavelength is limited by clinically relevant imaging depth and surrounding chromophores, which could affect the choice of a photo-absorber [17,18]. Laser activation of PFCnDs in the near-infrared region, where the optical penetration is effective, was demonstrated by numerous inorganic and organic materials, including gold nanoparticles and indocyanine green (ICG) dyes [10,13,19].

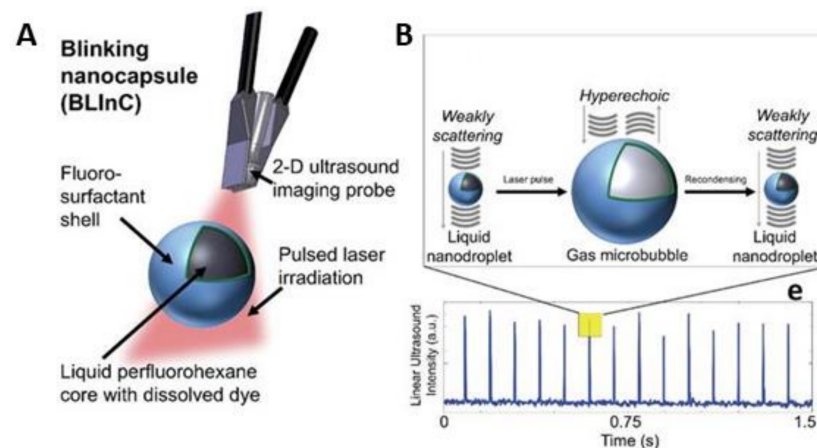


**Figure 1.** Laser-activated PFCnDs and their acoustic response over time. (A) A typical structure of PFCnDs comprising a liquid PFC core containing a photo-absorber stabilized by a surfactant shell. (B) Activating and deactivating PFCnDs in response to pulsed-laser irradiation and their corresponding ultrasound signals over time. Reprinted with permission from [20].

For the perfluorocarbon core, its type and boiling point can impact the activation and deactivation properties of the agents [9,11,21–23]. Nanodroplets with a low boiling point PFC (e.g., perfluorobutane) were shown to improve phase-changing efficiency compared to that of other higher boiling point PFCnDs. In other words, PFCnDs with a lower boiling point PFC core can be activated with lower energy at the same imaging depth or the same energy at the deeper imaging depth. When their boiling point is lower than surrounding physiological temperature ( $37^\circ\text{C}$ ) of the body, postactivated PFCnDs could remain as gaseous bubbles, not condensing back to the original liquid state. If the PFCnDs are constructed with a high boiling point PFC, the vaporized gas-filled PFCnDs can recondense, which allows them to be activated and deactivated again and again. For example, Figure 1B shows the temporal dynamics of PFCnDs containing perfluorohexane with a boiling point of  $56^\circ\text{C}$ . Thus, they can vaporize and recondense, which provides repeatable high US/PA contrast over a course of laser irradiation. Before optical activation, the PFCnDs remaining at the liquid state produce little ultrasound echoes. Once activated via pulsed laser illumination, the PFCnDs immediately vaporize and become gaseous microbubbles, generating hyperechoic ultrasound signals until they recondense. In addition, repeatable volumetric expansion makes this agent photoacoustically attractive, as high-contrast photoacoustic signals can be produced from the vaporization event.

This unique, repeated phase-changing property of high-boiling-point PFCnDs showed promising capabilities in US/PA imaging and therapeutic applications, including contrast-enhanced imaging, super-resolution imaging, extravascular tumor imaging, blood-brain barrier opening, and more. To capture rapidly changing dynamics of the PFCnDs and to support various imaging modes, relevant imaging algorithms and system configurations were explored. Overall, in this paper, “imaging”-related conditions, methods, and applications of optically triggered PFCnDs are the focus. This paper first discusses the acti-

vation and deactivation properties of laser-activated PFCnDs and introduces recent US/PA imaging approaches with this novel agent. Integrated laser and ultrasound system setups appropriate for imaging of PFCnDs are discussed too. Last section briefly summarizes diagnostic and therapeutic trends for applications.

## 2. Activation and Deactivation of Laser-Activated PFCnDs

Activation and deactivation (in other words, vaporization and recondensation) of the laser-activated PFCnDs are controlled by a combined function of many factors, including perfluorocarbon type, droplet size, local optical fluence, and amount of dye encapsulated [7,8,21,22,24–28]. A boiling point of perfluorocarbon core relative to surrounding physiological temperature (37 °C) is one of critical factors on both activation and deactivation of the PFCnDs. Higher optical fluence is generally needed to activate PFCnDs with a higher boiling point PFC. Table 1 summarizes the boiling points of selected perfluorocarbons used for PFCnDs.

**Table 1.** Boiling points of selected PFCs user for PFCnDs.

Perfluorocarbon Name (Chemical Formular)	Boiling Point (°C)
Perfluorooctylbromide (C <sub>8</sub> F <sub>17</sub> Br)	143
Perfluorooctane (C <sub>8</sub> F <sub>18</sub> )	99–106
Perfluorohexane (C <sub>6</sub> F <sub>14</sub> )	58–60
Perfluoropentane (C <sub>5</sub> F <sub>12</sub> )	28–30
Perfluorobutane (C <sub>4</sub> F <sub>10</sub> )	−1.7

For optical activation, pulsed-laser irradiation enables vaporization of laser-activated PFCnDs. The suspended plasmonic nanoparticles or dyes encapsulated in the droplet generate the heat and pressure, leading to vaporization of the PFC liquid core [7,10]. Wilson et al. showed that photoacoustic signals from vaporization comes first and subsequent thermal expansion is followed over a course of laser pulses [10]. Here, their PFCnDs are constructed with a low boiling point PFC (e.g., perfluoropentane in this study), only one-time activation is available at the beginning of laser irradiation, producing high-contrast photoacoustic signals. Relatively weaker photoacoustic signals are then generated during a series of following thermal expansion.

Activating deep and/or small PFCnDs is, however, challenging, which may require the optical fluence exceeding the American National Standards Institute safety limit for successful activation. Thus, to lower the optical activation threshold, Arnal et al. suggested sono-photoacoustic (SPA) imaging that synchronously combines acoustic and laser pulses [29,30]. To have both acoustic and laser pulses at the depth of interest and at the same time, the acoustic pulse is sent first as it is much slower than the laser pulse. Depending on the depth of interest, a traveling depth can be precalculated, and thus, the time delay between acoustic and laser pulses can be determined. With this approach, they were able to synchronize acoustic and optical activation pulses, which substantially lowered the PFCnD activation threshold. In addition, to cancel out unwanted linear photoacoustic sources and acoustic scatters, they specifically designed an imaging sequence with four successive ultrasound transmissions with alternating polarities. Similar concept was utilized for inertial cavitation-based sonoporation for tumor therapy [31]. More recently, Li et al. improved the SPA imaging sequence by applying focused and steered ultrasound beams, which enables highly localized activation of PFCnDs [32].

Perfluorohexane and perfluoropentane are commonly used materials for laser-activated PFCnDs. Compared to that of their similar vaporization properties, their recondensation behaviors are indeed more different [23]. As shown in Table 1, a boiling point of perfluorohexane is higher than a body temperature, and thus, perfluorohexane nanodroplets (PFHnDs) can condense back to their original liquid form after vaporization, as shown in Figure 2. However, perfluoropentane nanodroplets (PFpnDs) could remain as gaseous

bubbles. Therefore, PFHnDs can repeatedly vaporize and recondense, providing repeated strong photoacoustic contrast and uniquely enabling novel ultrasound imaging methods.

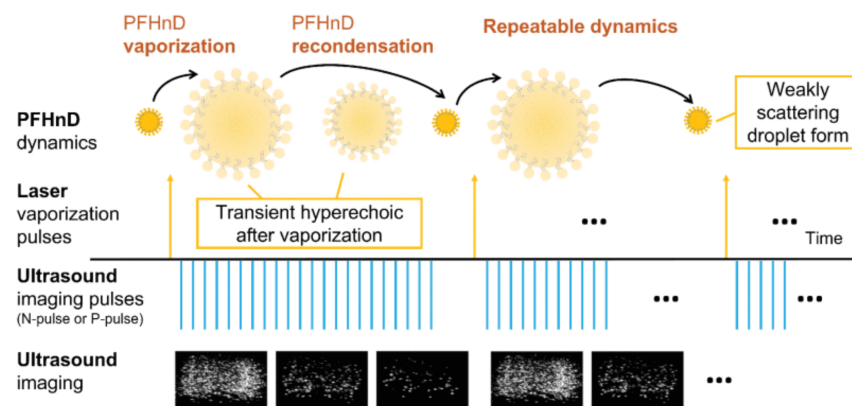


**Figure 2.** Vaporization and recondensation of laser-activated PFHnDs. Postactivated PFHnDs are imaged with ultrasound and exhibit repeated decaying ultrasound signals over period. Reprinted with permission from [33].

PFHnD's recondensation time is, however, relatively transient, ranging from several to hundreds of milliseconds [16,22,33]. Zhu et al. found that the phase of ultrasound imaging pulse impacts the recondensation dynamics [33]. For example, if the initial part of transmit pulse is rarefactional rather than compressional, it was experimentally shown that the corresponding recondensation time is extended, and the signal-to-noise ratio is improved as well. Another important property of droplet recondensation is its stochasticity. As noted earlier, the recondensation process is complex and a combined function of droplet size, local laser fluence, amount of dye, shell composition, and imaging conditions, along with local temperature, pressure, and viscoelasticity. Therefore, isolation of randomly recondensing individual droplet is feasible, which enabled super-resolution imaging [22,24].

### 3. Ultrasound and Photoacoustic Imaging of Laser-Activated PFCnDs

Laser-activated PFCnDs are a dual-modality agent offering both ultrasonic and photoacoustic contrast [5,10,13,15,18,34,35]. Most US/PA imaging studies with laser-activated PFCnDs utilized two types of PFCnDs: PFPnDs and PFHnDs. Both as liquid nanodroplets are not easily ultrasonically detectable before optical activation. In response to laser irradiation, the encapsulated dyes or nanoparticles absorb optical energy, producing heat and photoacoustic pressures. This process eventually initiates a liquid-to-gas transition of PFCnDs, resulting in vaporization or volumetric expansion of the droplets. For PFPnDs, after vaporization, they persist their gaseous state. Here, three contrast mechanisms can be appreciated with laser activation of PFPnDs. Volumetric expansion and thermal expansion produce photoacoustic signals, and vaporized gas-filled bubbles can provide high-contrast in ultrasound. As shown in Figure 3, the first vaporization event yields the strongest photoacoustic signal, and the following thermal expansion results in relatively weaker photoacoustic signals over a course of laser pulses.

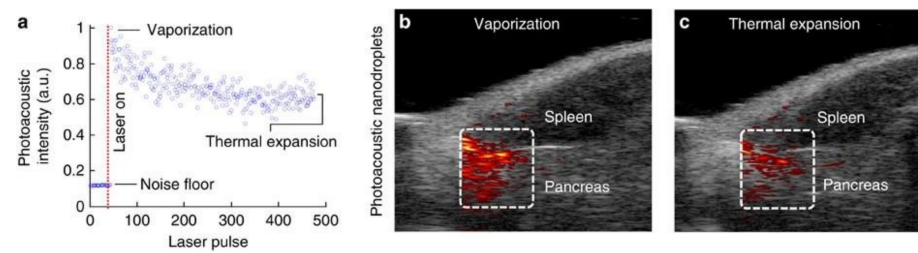


**Figure 3.** In vivo US/PA imaging experiments demonstrating vaporization and thermal expansion-induced photoacoustic signals over a course of laser pulses. (a) Mean photoacoustic signals before and after laser irradiation, (b) vaporization signal, and (c) thermal expansion signal. Image (b,c) are 20.4 mm wide by 12.8 mm tall, and ultrasound signals are displayed using a 20-dB scale. Reprinted under permission from [10].

Exploiting higher-boiling-point PFCnDs (e.g., PFHnDs) offers an ability to reactivate the agent because of their recondensation after vaporization, which enables extended imaging methods, such as background-free contrast-enhanced ultrasound and super-resolution ultrasound imaging [16,20,22,24]. A lifetime of vaporized PFHnDs is known to range from several to hundreds of milliseconds, which is relatively transient to utilize them for prolonged high-contrast imaging. To localize the PFHnDs, autocorrelation of a set of ultrasound images containing several events of droplet vaporization and recondensation was suggested. Later, Yoon et al. proposed a computationally-efficient PFHnD-localization algorithm for real-time in vivo imaging [16]. By incorporating the periodic nature of droplet vaporization and recondensation in response to laser irradiation, they developed a formula that can map a probability of droplet existence on the image and showed successful differentiation of lymph node of a mouse model from surrounding tissue, as shown in Figure 4. From the temporal ultrasound profile measured on a pixel containing PFHnDs, vaporization and recondensation behaviors are observable, but not as much clear as phantom imaging in their study [16].

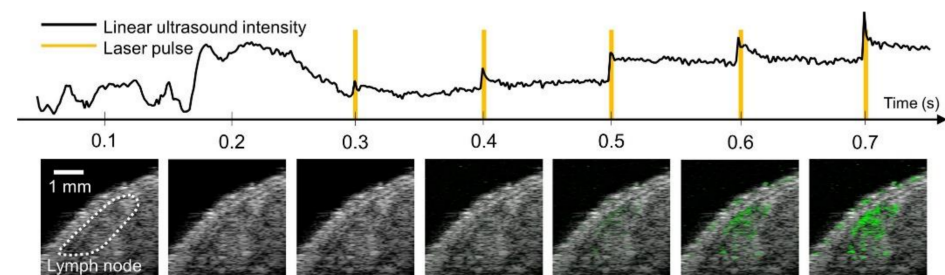


**Figure 4.** In vivo contrast-enhanced ultrasound imaging of murine lymph node processed with a PFHnD-localization algorithm over time. Laser pulses start activating the PFHnDs at 0.3 s. Reprinted under permission from [16].

Compared to that of microbubble-based ultrasound super-resolution imaging, laser-activated PFCnD-based super-resolution methods are relatively new. Luke et al. found that the recondensation of PFHnDs is a stochastic process [22]. Depending on many factors, including droplet size, local fluence, and absorbance of dye, the recondensation time of PFHnDs varies randomly. This randomized recondensation of PFHnDs offers a chance to isolate individual droplet if imaging rate is fast enough to capture each recondensation event. Their super-resolution approach shows the 8-fold improvement in spatial resolution over conventional ultrasound. Later, Yoon et al. applied ultrafast plane-wave ultrasound to the super-resolution imaging technique to increase the acquisition frame rate, and also to enhance the image signal-to-noise ratio through temporal compounding [24]. They demonstrated that the resolution improves as a function of the number of frames compounded.

US/PA imaging of laser-activated PFHnDs necessitates integrated laser and ultrasound systems and relevant imaging sequences to reach their full potential. Combined multiwavelength photoacoustic and plane-wave ultrasound imaging was suggested to support imaging of transient phase-change contrast agents [36]. As a result, US/PA signals from the PFHnDs were measured as a function of both optical wavelength and time, capable of demonstrating the optical wavelength dependency of US/PA imaging and temporal dynamics of PFHnDs simultaneously. However, optical wavelength tuning is too slow to produce real-time images with their approach. Recently, Jeng et al. achieved 50-Hz US/PA imaging rate with sequential spectroscopic laser irradiation [37]. Although their system was not demonstrated with phase-change contrast agents, their high-laser-pulse repetition rate should be beneficial to in vivo imaging.

As conventional microbubbles (typically 1–10  $\mu\text{m}$  diameter) cannot leave the blood vessels, they are unable to target or visualize extravascular pathology outside of the vascular space [9,12,38,39]. However, due to the submicrometer size of PFCnDs, the PFCnDs can extravasate from leaky cancerous neovasculature and accumulate in tumors by the enhanced permeability and retention (EPR) effect. As a result, they can provide an opportunity for extravascular US/PA imaging of cancer. To achieve reliable extravascular imaging, producing consistently small, monodisperse PFCnDs is critical. Paproski et al. produced the droplets smaller than 200 nm with all organic materials and showed successful accumulation of the droplets in their tumor model [14]. Additionally, US/PA imaging was able to identify their nanodroplets specifically as shown in Figure 5. Yarmoska et al. demonstrated that increased molar percentage of lipid reduces the size and size variance of PFCnDs [12]. With their nanodroplets, they found substantial photoacoustic contrast enhancement within the primary tumor region of the mouse after 24-h post injection.

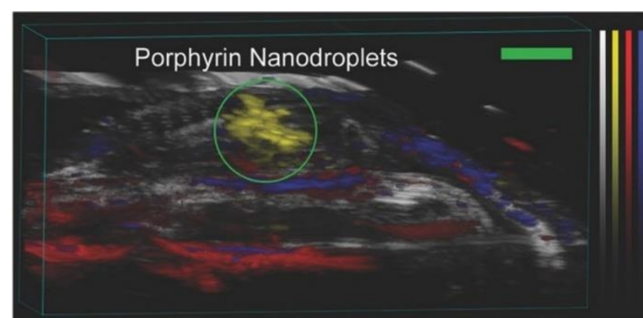


**Figure 5.** In vivo three-dimensional ultrasound and photoacoustic imaging of porphyrin nanodroplets. Yellow, red, and blue photoacoustic signals represent porphyrin nanodroplets, oxygenated hemoglobin, and deoxygenated hemoglobin, respectively. Green scale bar represents 3-mm length. Reprinted under permission from [14].

Sono-photoacoustic imaging synchronously combines acoustic and optical triggers to lower the overall activation threshold of PFCnDs, and thus, enhances the sensitivity for deeper imaging with smaller agents [30,32,40]. To obtain background-free droplet-localized images, the authors used a pulse inversion technique for acoustic pulses applied for droplet activation. Thus, with their SPA imaging sequence, specific detection of nanodroplets is possible under low concentration. Later, SPA imaging becomes highly localized with the addition of acoustic beam focusing/steering [32]. As demonstrated in Figure 6, complex patterns can be programmed and drawn with the SPA imaging sequence under acoustic and optical safety limits.

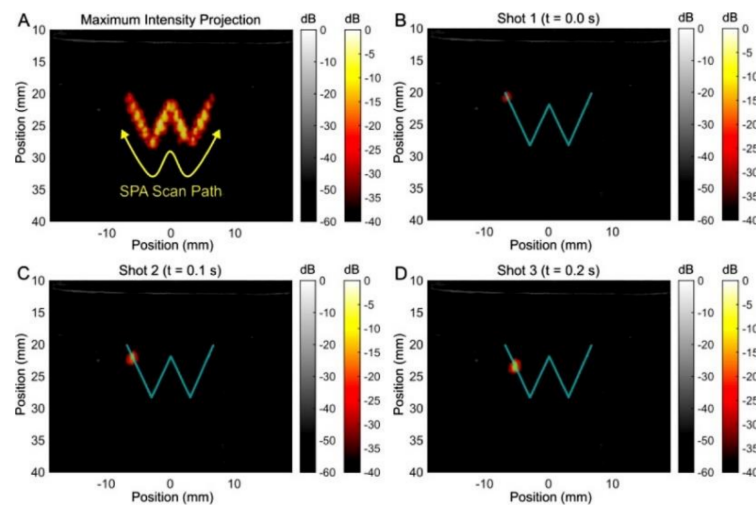


**Figure 6.** Demonstrated results of steered, localized SPA activation along an arbitrary complex path to draw a letter ‘W’. (A) Final SPA image represented with maximum intensity projection. (B–D) show individual SPA activation point at 0.0, 0.1, and 0.2 s, respectively. Reprinted under permission from [32].

#### 4. Therapeutic and Theranostic Applications with Laser-Activated PFCnDs

Our primary focus on this paper is “imaging” of laser-activated PFCnDs for improved identification and localization of diseases, but these agents are indeed very attractive therapeutic and theranostic tools for various US/PA applications [1,2,6,18,31,34,41,42]. PFCnDs are in general capable of carrying therapeutic drugs or other particles. They are also useful in photothermal and photodynamic therapies. In addition, PFCnDs can contain oxygen to alleviate hypoxia-related resistance in cancer therapies. Yang et al. showed their carbon nanoparticle-based PFHnDs can produce high US/PA contrast, as well as photothermally ablate cancer cells *in vivo* [15]. Longitudinal US/PA images of mouse lymph node after their nanodroplet injection are shown in Figure 7A. Ultrasound and contrast mode combinations are presented in Figure 7B, which demonstrates the ability of their agents for nonlinear harmonic imaging.

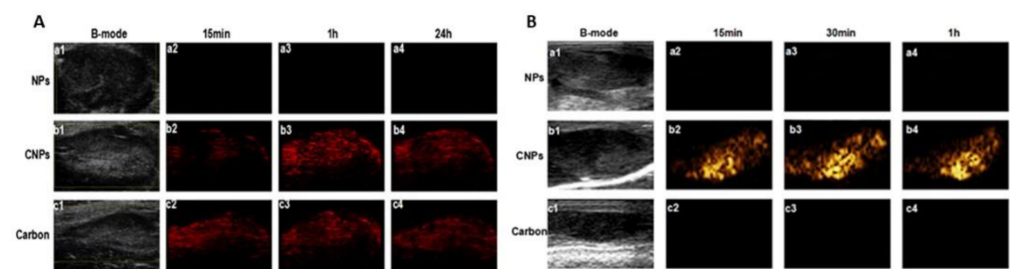


**Figure 7.** (A) Photoacoustic and (B) contrast-enhanced imaging of *in vivo* mouse lymph node with the carbon nanoparticles-incorporated nanodroplets (CNPs) and controls at different time points. Reprinted under permission from [15].

PFCnDs can be useful in neurological applications [43,44]. Focused ultrasound with microbubbles was investigated as an effective tool for blood brain barrier (BBB) opening to enable monitoring and treatment of neurological diseases [45]. The use of PFCnDs is another possible method that can open the BBB noninvasively. With low-boiling-point PFCnDs, acoustically-activated PFCnDs remain in their gaseous state, capable of producing comparable BBB opening effects to that of traditional microbubbles [46]. More recently, Hallam et al. showed laser-activated PFCnDs as an alternative BBB opening tool with PFHnDs, which can be selectively and repeatedly vaporize at the specific optical wavelength [43].

Wavelength-specific activation is achievable with laser-activated PFCnDs depending on the choice of optical absorbers, which enables multiplexed imaging and therapy. Multiplexed imaging is capable of molecularly and simultaneously targeting and visualizing multiple functional cells and parameters, which is desired for diagnosis of complex disease like cancer [47]. Recently, Santiesteban et al. showed that laser-activated PFCnDs can be color-coded at 680 and 1064 nm [48]. They demonstrated in situ and in vivo that their PFCnDs can be selectively activated in response to laser irradiation at corresponding wavelengths. Figure 8 shows independent multiplexed imaging results of two PFCnDs activated at different optical wavelengths. They showed that intradermally and intravenously injected PFCnDs are distinguishable because of their optical selectivity.

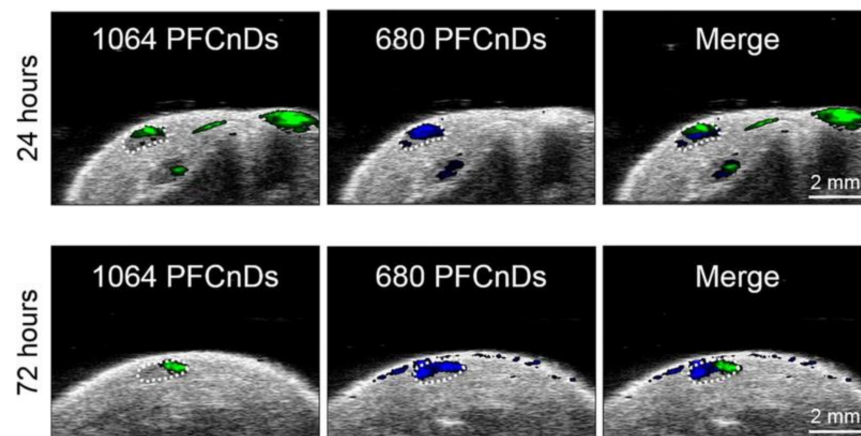


**Figure 8.** In vivo US/PA processed images presenting multiplexed PFCnDs injected both intradermally (green) and intravenously (blue). Twenty-four- or 72-h time points refer to intradermally-injected 1064 PFCnDs. US/PA imaging was performed immediately after intravenous injection of 680 PFCnDs. Reprinted under permission from [48].

## 5. Discussion

So far, we discussed various approaches enhancing image contrast with PFCnDs. To achieve further improved imaging contrast, engineering advanced and functional PFCnDs would be critical. For example, PFCnDs can be surface-modified for molecular targeting of cancer cells [49], and the associated imaging contrast can then be specific to the region of interest, potentially providing localized contrast, and thus, improving diagnostic capabilities. Moreover, image-guided delivery of therapeutics using PFCnDs recently showed that PFCnDs have a capacity for simultaneous drug delivery and ultrasound monitoring, indicating that localized treatment and imaging of cancer with PFCnDs may be feasible in the future [50]. Furthermore, PFCnDs can be incorporated into other medical imaging modalities, including magnetic resonance imaging (MRI) as a multimodal agent [51]. Wu et al. demonstrated that their  $^{19}\text{F}$  MRI approach with ligand-targeted PFCnDs can effectively detect tumors, sense oxygenation, and monitor therapeutic progress [52].

On the other hand, for the successful clinical translation of imaging methods with PFCnDs, their biocompatibility should be thoroughly investigated, as in many cases, the imaging capability and the biosafety of the PFCnDs are in a tradeoff relation [53]. Every component of the droplet, including a photo-absorber, needs to be nontoxic, biodegradable, and thus, FDA-approved. For example, clinically-proved ICG dye was demonstrated to be employed for optically-triggered PFCnDs with high-imaging-contrast [13]. In addition, PFCnDs should clearly answer the concerns on long-term toxicity and bioeffects. Combining inorganic and organic components for balancing both imaging capability and biosafety was attempted for constructing PFCnDs, and they are successfully demonstrated in vivo [17].

## 6. Conclusions

This review paper focused on US/PA imaging associated with laser-activated PFCnDs to introduce how various imaging methods can be engineered to enhance diagnostic capabilities with the use of PFCnDs. As other medical imaging modalities, US/PA imaging is limited by its fundamental and physical resolution and contrast. Repeated activation and deactivation of PFCnDs enabled contrast-enhanced ultrasound and super-resolution ultrasound imaging, which allow for imaging beyond the traditional limits. Sono-photoacoustic imaging enables deep, localized activation of PFCnDs under the safety limits. With these technological improvements, US/PA imaging of PFCnDs are becoming a more versatile imaging tool. Previously developed imaging methods will be possibly combined with multiplexed approaches, which will make these agents more functional. More preclinical and clinical trials are needed for clinical translation at the end, which are on-going activities to demonstrate biological safety and diagnostic/therapeutic efficacy with laser-activated PFCnDs.

**Funding:** The present research was supported by the research fund of Dankook University in 2021.

**Conflicts of Interest:** The authors declare no conflict of interest.

## References

1. Sheeran, P.S.; Dayton, P.A. Phase-Change Contrast Agents for Imaging and Therapy. *Curr. Pharm. Des.* **2012**, *18*, 2152–2165. [[CrossRef](#)]
2. Dayton, P.A.; Zhao, S.; Bloch, S.H.; Schumann, P.; Penrose, K.; Matsunaga, T.O.; Zutshi, R.; Doinikov, A.; Ferrara, K.W. Application of Ultrasound to Selectively Localize Nanodroplets for Targeted Imaging and Therapy. *Mol. Imaging* **2006**, *5*, 160–174. [[CrossRef](#)]
3. Zullino, S.; Argenziano, M.; Stura, I.; Guiot, C.; Cavalli, R. From Micro- to Nano-Multifunctional Theranostic Platform: Effective Ultrasound Imaging Is Not Just a Matter of Scale. *Mol. Imaging* **2018**, *17*, 1536012118778216. [[CrossRef](#)]
4. Loskutova, K.; Grishenkov, D.; Ghorbani, M. Review on Acoustic Droplet Vaporization in Ultrasound Diagnostics and Therapeutics. *BioMed Res. Int.* **2019**, *2019*, 9480193. [[CrossRef](#)]
5. Lin, S.; Shah, A.; Hernández-Gil, J.; Stanziola, A.; Harriss, B.I.; Matsunaga, T.O.; Long, N.; Bamber, J.; Tang, M.-X. Optically and Acoustically Triggerable Sub-Micron Phase-Change Contrast Agents for Enhanced Photoacoustic and Ultrasound Imaging. *Photoacoustics* **2017**, *6*, 26–36. [[CrossRef](#)]
6. Rapoport, N. Phase-Shift, Stimuli-Responsive Perfluorocarbon Nanodroplets for Drug Delivery to Cancer. *Wiley Interdiscip. Rev. Nanomed. Nanobiotechnol.* **2012**, *4*, 492–510. [[CrossRef](#)]
7. Strohm, E.; Rui, M.; Gorelikov, I.; Matsuura, N.; Kolios, M. Vaporization of Perfluorocarbon Droplets Using Optical Irradiation. *Biomed. Opt. Express* **2011**, *2*, 1432–1442. [[CrossRef](#)]
8. Kripfgans, O.D.; Fabiilli, M.L.; Carson, P.L.; Fowlkes, J.B. On the Acoustic Vaporization of Micrometer-Sized Droplets. *J. Acoust. Soc. Am.* **2004**, *116*, 272–281. [[CrossRef](#)] [[PubMed](#)]
9. Sheeran, P.S.; Wong, V.P.; Luois, S.; McFarland, R.J.; Ross, W.D.; Feingold, S.; Matsunaga, T.O.; Dayton, P.A. Decafluorobutane as a Phase-Change Contrast Agent for Low-Energy Extravascular Ultrasonic Imaging. *Ultrasound Med. Biol.* **2011**, *37*, 1518–1530. [[CrossRef](#)] [[PubMed](#)]
10. Wilson, K.; Homan, K.; Emelianov, S. Biomedical Photoacoustics beyond Thermal Expansion Using Triggered Nanodroplet Vaporization for Contrast-Enhanced Imaging. *Nat. Commun.* **2012**, *3*, 618. [[CrossRef](#)] [[PubMed](#)]
11. Matsunaga, T.O.; Sheeran, P.S.; Luois, S.; Streeter, J.E.; Mullin, L.B.; Banerjee, B.; Dayton, P.A. Phase-Change Nanoparticles Using Highly Volatile Perfluorocarbons: Toward a Platform for Extravascular Ultrasound Imaging. *Theranostics* **2012**, *2*, 1185–1198. [[CrossRef](#)]
12. Yarmoska, S.K.; Yoon, H.; Emelianov, S.Y. Lipid Shell Composition Plays a Critical Role in the Stable Size Reduction of Perfluorocarbon Nanodroplets. *Ultrasound Med. Biol.* **2019**, *45*, 1489–1499. [[CrossRef](#)]
13. Hannah, A.; Luke, G.; Wilson, K.; Homan, K.; Emelianov, S. Indocyanine Green-Loaded Photoacoustic Nanodroplets: Dual Contrast Nanoconstructs for Enhanced Photoacoustic and Ultrasound Imaging. *ACS Nano* **2014**, *8*, 250–259. [[CrossRef](#)]
14. Paproski, R.J.; Forbrich, A.; Huynh, E.; Chen, J.; Lewis, J.D.; Zheng, G.; Zemp, R.J. Porphyrin Nanodroplets: Sub-Micrometer Ultrasound and Photoacoustic Contrast Imaging Agents. *Small* **2016**, *12*, 371–380. [[CrossRef](#)] [[PubMed](#)]
15. Yang, L.; Cheng, J.; Chen, Y.; Yu, S.; Liu, F.; Sun, Y.; Chen, Y.; Ran, H. Phase-Transition Nanodroplets for Real-Time Photoacoustic/Ultrasound Dual-Modality Imaging and Photothermal Therapy of Sentinel Lymph Node in Breast Cancer. *Sci. Rep.* **2017**, *7*, 45213. [[CrossRef](#)]
16. Yoon, H.; Yarmoska, S.K.; Hannah, A.S.; Yoon, C.; Hallam, K.A.; Emelianov, S.Y. Contrast-Enhanced Ultrasound Imaging in Vivo with Laser-Activated Nanodroplets. *Med. Phys.* **2017**, *44*, 3444–3449. [[CrossRef](#)] [[PubMed](#)]
17. Santiesteban, D.Y.; Dumani, D.S.; Profili, D.; Emelianov, S.Y. Copper Sulfide Perfluorocarbon Nanodroplets as Clinically Relevant Photoacoustic/Ultrasound Imaging Agents. *Nano Lett.* **2017**, *17*, 5984–5989. [[CrossRef](#)] [[PubMed](#)]

18. Tang, W.; Yang, Z.; Wang, S.; Wang, Z.; Song, J.; Yu, G.; Fan, W.; Dai, Y.; Wang, J.; Shan, L.; et al. Organic Semiconducting Photoacoustic Nanodroplets for Laser-Activatable Ultrasound Imaging and Combinational Cancer Therapy. *ACS Nano* **2018**, *12*, 2610–2622. [[CrossRef](#)]
19. Dove, J.D.; Mountford, P.A.; Murray, T.W.; Borden, M.A. Engineering Optically Triggered Droplets for Photoacoustic Imaging and Therapy. *Biomed. Opt. Express* **2014**, *5*, 4417–4427. [[CrossRef](#)]
20. Hannah, A.S.; Luke, G.P.; Emelianov, S.Y. Blinking Phase-Change Nanocapsules Enable Background-Free Ultrasound Imaging. *Theranostics* **2016**, *6*, 1866–1876. [[CrossRef](#)]
21. Yu, J.; Chen, X.; Villanueva, F.S.; Kim, K. Vaporization and Recondensation Dynamics of Indocyanine Green-Loaded Perfluoropentane Droplets Irradiated by a Short Pulse Laser. *Appl. Phys. Lett.* **2016**, *109*, 243701. [[CrossRef](#)]
22. Luke, G.P.; Hannah, A.S.; Emelianov, S.Y. Super-Resolution Ultrasound Imaging in Vivo with Transient Laser-Activated Nanodroplets. *Nano Lett.* **2016**, *16*, 2556–2559. [[CrossRef](#)] [[PubMed](#)]
23. Van Namen, A.; Jandhyala, S.; Jordan, T.; Luke, G. *Repeated Acoustic Vaporization of Perfluorohexane Nanodroplets for Contrast-Enhanced Ultrasound Imaging*; IEEE: Manhattan, NY, USA, 2021.
24. Yoon, H.; Hallam, K.A.; Yoon, C.; Emelianov, S.Y. Super-Resolution Imaging With Ultrafast Ultrasound Imaging of Optically Triggered Perfluorohexane Nanodroplets. *IEEE Trans. Ultrason. Ferroelectr. Freq. Control* **2018**, *65*, 2277–2285. [[CrossRef](#)] [[PubMed](#)]
25. Shpak, O.; Verweij, M.; Vos, H.J.; de Jong, N.; Lohse, D.; Versluis, M. Acoustic Droplet Vaporization Is Initiated by Superharmonic Focusing. *Proc. Natl. Acad. Sci. USA* **2014**, *111*, 1697. [[CrossRef](#)]
26. Wu, Q.; Mannaris, C.; May, J.P.; Bau, L.; Polydorou, A.; Ferri, S.; Carugo, D.; Evans, N.D.; Stride, E. Investigation of the Acoustic Vaporization Threshold of Lipid-Coated Perfluorobutane Nanodroplets Using Both High-Speed Optical Imaging and Acoustic Methods. *Ultrasound Med. Biol.* **2021**, *47*, 1826–1843. [[CrossRef](#)]
27. Rojas, J.D.; Dayton, P.A. Optimizing Acoustic Activation of Phase Change Contrast Agents With the Activation Pressure Matching Method: A Review. *IEEE Trans. Ultrason. Ferroelectr. Freq. Control* **2017**, *64*, 264–272. [[CrossRef](#)]
28. Aliabouzar, M.; Kumar, K.N.; Sarkar, K. Effects of Droplet Size and Perfluorocarbon Boiling Point on the Frequency Dependence of Acoustic Vaporization Threshold. *J. Acoust. Soc. Am.* **2019**, *145*, 1105–1116. [[CrossRef](#)]
29. Arnal, B.; Perez, C.; Wei, C.-W.; Xia, J.; Lombardo, M.; Pelivanov, I.; Matula, T.J.; Pozzo, L.D.; O'Donnell, M. Sono-Photoacoustic Imaging of Gold Nanoemulsions: Part I. Exposure Thresholds. *Photoacoustics* **2015**, *3*, 3–10. [[CrossRef](#)] [[PubMed](#)]
30. Arnal, B.; Wei, C.-W.; Perez, C.; Nguyen, T.-M.; Lombardo, M.; Pelivanov, I.; Pozzo, L.D.; O'Donnell, M. Sono-Photoacoustic Imaging of Gold Nanoemulsions: Part II. Real Time Imaging. *Photoacoustics* **2015**, *3*, 11–19. [[CrossRef](#)]
31. Liu, W.-W.; Huang, S.-H.; Li, P.-C. Synchronized Optical and Acoustic Droplet Vaporization for Effective Sonoporation. *Pharmaceutics* **2019**, *11*, 279. [[CrossRef](#)]
32. Li, D.S.; Jeng, G.-S.; Pitre, J.J.; Kim, M.; Pozzo, L.D.; O'Donnell, M. Spatially Localized Sono-Photoacoustic Activation of Phase-Change Contrast Agents. *Photoacoustics* **2020**, *20*, 100202. [[CrossRef](#)]
33. Zhu, Y.I.; Yoon, H.; Zhao, A.X.; Emelianov, S.Y. Leveraging the Imaging Transmit Pulse to Manipulate Phase-Change Nanodroplets for Contrast-Enhanced Ultrasound. *IEEE Trans. Ultrason. Ferroelectr. Freq. Control* **2019**, *66*, 692–700. [[CrossRef](#)]
34. Yang, C.; Zhang, Y.; Luo, Y.; Qiao, B.; Wang, X.; Zhang, L.; Chen, Q.; Cao, Y.; Wang, Z.; Ran, H. Dual Ultrasound-Activatable Nanodroplets for Highly-Penetrative and Efficient Ovarian Cancer Theranostics. *J. Mater. Chem. B* **2020**, *8*, 380–390. [[CrossRef](#)]
35. Hannah, A.S.; VanderLaan, D.; Chen, Y.-S.; Emelianov, S.Y. Photoacoustic and Ultrasound Imaging Using Dual Contrast Perfluorocarbon Nanodroplets Triggered by Laser Pulses at 1064 nm. *Biomed. Opt. Express* **2014**, *5*, 3042–3052. [[CrossRef](#)]
36. Yoon, H.; Emelianov, S.Y. Combined Multiwavelength Photoacoustic and Plane-Wave Ultrasound Imaging for Probing Dynamic Phase-Change Contrast Agents. *IEEE Trans. Biomed. Eng.* **2019**, *66*, 595–598. [[CrossRef](#)]
37. Jeng, G.-S.; Li, M.-L.; Kim, M.; Yoon, S.J.; Pitre, J.J.; Li, D.S.; Pelivanov, I.; O'Donnell, M. Real-Time Interleaved Spectroscopic Photoacoustic and Ultrasound (PAUS) Scanning with Simultaneous Fluence Compensation and Motion Correction. *Nat. Commun.* **2021**, *12*, 716. [[CrossRef](#)]
38. Rojas, J.D.; Dayton, P.A. In Vivo Molecular Imaging Using Low-Boiling-Point Phase-Change Contrast Agents: A Proof of Concept Study. *Ultrasound Med. Biol.* **2019**, *45*, 177–191. [[CrossRef](#)] [[PubMed](#)]
39. Li, D.S.; Schneewind, S.; Bruce, M.; Khaing, Z.; O'Donnell, M.; Pozzo, L. Spontaneous Nucleation of Stable Perfluorocarbon Emulsions for Ultrasound Contrast Agents. *Nano Lett.* **2019**, *19*, 173–181. [[CrossRef](#)] [[PubMed](#)]
40. Li, D.S.; Yoon, S.J.; Pelivanov, I.; Frenz, M.; O'Donnell, M.; Pozzo, L.D. Polypyrrole-Coated Perfluorocarbon Nanoemulsions as a Sono-Photoacoustic Contrast Agent. *Nano Lett.* **2017**, *17*, 6184–6194. [[CrossRef](#)] [[PubMed](#)]
41. Qin, D.; Zhang, L.; Zhu, H.; Chen, J.; Wu, D.; Bouakaz, A.; Wan, M.; Feng, Y. A Highly Efficient One-for-All Nanodroplet for Ultrasound Imaging-Guided and Cavitation-Enhanced Photothermal Therapy. *Int. J. Nanomed.* **2021**, *16*, 3105–3119. [[CrossRef](#)] [[PubMed](#)]
42. Guo, R.; Xu, N.; Liu, Y.; Ling, G.; Yu, J.; Zhang, P. Functional Ultrasound-Triggered Phase-Shift Perfluorocarbon Nanodroplets for Cancer Therapy. *Ultrasound Med. Biol.* **2021**, *47*, 2064–2079. [[CrossRef](#)]
43. Hallam, K.A.; Donnelly, E.M.; Karpouk, A.B.; Hartman, R.K.; Emelianov, S.Y. Laser-Activated Perfluorocarbon Nanodroplets: A New Tool for Blood Brain Barrier Opening. *Biomed. Opt. Express* **2018**, *9*, 4527–4538. [[CrossRef](#)] [[PubMed](#)]
44. Jing, B.; Kashyap, E.P.; Lindsey, B.D. Transcranial Activation and Imaging of Low Boiling Point Phase-Change Contrast Agents through the Temporal Bone Using an Ultrafast Interframe Activation Ultrasound Sequence. *Med. Phys.* **2020**, *47*, 4450–4464. [[CrossRef](#)] [[PubMed](#)]

45. Hynynen, K.; McDannold, N.; Vykhodtseva, N.; Jolesz, F.A. Non-Invasive opening of BBB by focused ultrasound. In *Proceedings of the Brain Edema XII*; Kuroiwa, T., Baethmann, A., Czernicki, Z., Hoff, J.T., Ito, U., Katayama, Y., Marmarou, A., Mendelow, B.A.D., Reulen, H.-J., Eds.; Springer: Vienna, Austria, 2003; pp. 555–558.
46. Chen, C.C.; Sheeran, P.S.; Wu, S.-Y.; Olumolade, O.O.; Dayton, P.A.; Konofagou, E.E. Targeted Drug Delivery with Focused Ultrasound-Induced Blood-Brain Barrier Opening Using Acoustically-Activated Nanodroplets. *J. Control. Release* **2013**, *172*, 795–804. [[CrossRef](#)]
47. Heinzmann, K.; Carter, L.M.; Lewis, J.S.; Aboagye, E.O. Multiplexed Imaging for Diagnosis and Therapy. *Nat. Biomed. Eng.* **2017**, *1*, 697–713. [[CrossRef](#)] [[PubMed](#)]
48. Santiesteban, D.Y.; Hallam, K.A.; Yarmoska, S.K.; Emelianov, S.Y. Color-Coded Perfluorocarbon Nanodroplets for Multiplexed Ultrasound and Photoacoustic Imaging. *Nano Res.* **2019**, *12*, 741–747. [[CrossRef](#)] [[PubMed](#)]
49. Ishijima, A.; Minamihata, K.; Yamaguchi, S.; Yamahira, S.; Ichikawa, R.; Kobayashi, E.; Iijima, M.; Shibasaki, Y.; Azuma, T.; Nagamune, T.; et al. Selective Intracellular Vaporisation of Antibody-Conjugated Phase-Change Nano-Droplets in Vitro. *Sci. Rep.* **2017**, *7*, 44077. [[CrossRef](#)]
50. Spatarelu, C.-P.; Van Namen, A.; Luke, G.P. Optically Activatable Double-Drug-Loaded Perfluorocarbon Nanodroplets for On-Demand Image-Guided Drug Delivery. *ACS Appl. Nano Mater.* **2021**, *4*, 8026–8038. [[CrossRef](#)]
51. Koshkina, O.; Lajoinie, G.; Baldelli Bombelli, F.; Swider, E.; Cruz, L.J.; White, P.B.; Schweins, R.; Dolen, Y.; van Dintther, E.A.W.; van Riessen, N.K.; et al. Multicore Liquid Perfluorocarbon-Loaded Multimodal Nanoparticles for Stable Ultrasound and 19F MRI Applied to In Vivo Cell Tracking. *Adv. Funct. Mater.* **2019**, *29*, 1806485. [[CrossRef](#)]
52. Wu, L.; Liu, F.; Liu, S.; Xu, X.; Liu, Z.; Sun, X. Perfluorocarbons-Based (19)F Magnetic Resonance Imaging in Biomedicine. *Int. J. Nanomed.* **2020**, *15*, 7377–7395. [[CrossRef](#)]
53. Sheeran, P.S.; Matsuura, N.; Borden, M.A.; Williams, R.; Matsunaga, T.O.; Burns, P.N.; Dayton, P.A. Methods of Generating Submicrometer Phase-Shift Perfluorocarbon Droplets for Applications in Medical Ultrasonography. *IEEE Trans. Ultrason. Ferroelectr. Freq. Control* **2017**, *64*, 252–263. [[CrossRef](#)] [[PubMed](#)]